



Ashing temperature of lignite and mineral transition sequence

Boyang Wang^{a,b,*}, Miao Liu^c

^a Key Laboratory of Coalbed Methane Resources and Reservoir Formation Process, Ministry of Education, China University of Mining and Technology, Xuzhou 221116, China

^b School of Resources and Geosciences, China University of Mining and Technology, Xuzhou 221116, China

^c Daqing Oilfield Production Engineering and Researching Institute, Daqing Oil Field Co, Daqing 163453, China

ARTICLE INFO

Keywords:

Erlian Basin
Lignite
Minerals
Ashing temperature
AAEMS

ABSTRACT

To investigate the effect of non-mineral inorganics on the degree of ashing and determine the minerals in lignite, we performed selective leaching of amorphous materials in coal. Three kinds of lignite ash samples were prepared at < 200 °C, 500 °C and 815 °C, and the minerals and ash products were analyzed by X-ray diffraction, ash composition analysis and statistical modelling. The results suggest that the mineral types of the main coal seams of three sags in the Erlian Basin mainly comprise of clay minerals and quartz, of which clay minerals are mainly kaolinite, followed by mixed illite/smectite and illite. The increase in ashing temperature below 500 °C was found to not affect the mineral species, but it damages the clay minerals to various degrees, mainly kaolinite. Based on principal component analysis and multiple regression analysis, a prediction model was established for medium-temperature ash to obtain the low-temperature ash mineral composition. Erlian Basin lignite contains a large amount of alkali or alkaline earth elements (AAEMS), among which Ca, Na, and Mg cations react with organic oxygen-containing functional groups or other organic functional groups, whereas K is mainly hosted in clay minerals. The positive effect of AAEMS in non-mineral inorganics on the ash yield is higher than the negative effect of the increase in ashing temperature. Ca is an important element that controls the degree of ashing in low-temperature ashing below 500 °C. The effect of Mg on the degree of ashing is enhanced with increasing ashing temperature, but does not exceed that of Ca.

1. Introduction

Minerals are present in coal, which makes knowing the minerals in coal essential for coal processing and coal dressing (Li et al., 2017a, 2017b). The mineral content in coal is low, and its relation to the organic matter is complex, which complicates mineral identification in coal. Usually, the first step is to perform coal ashing to remove the organic matter and then analyze the residue. Currently, low-temperature ashing is the best method to separate minerals without changing the mineral species; furthermore, the lower the degree of metamorphism is, the easier the ashing (Ward, 1978; Harvey and Ruch, 1984; Harvey and Ruch, 1986; Ward, 1991; Ward, 1992; Ward and Taylor, 1996; Song, 2011). However, low-temperature ashing is complex and time consuming (24 to 50 h); moreover, oxygen plasma low-temperature ashing is inapplicable to lignite and peat because the non-mineral inorganics in coal can form NH₄SO₄ with organic sulfur and organic nitrogen as well as other substances that affect ashing. In addition, the proportion of non-mineral inorganics in low-rank coal is high (Benson and Holm, 1985; Cao and Li, 1994; Shang et al., 2016).

Currently, the mechanism by which non-mineral inorganics affect the ashing of coal needs to be analyzed, and the methods to efficiently and accurately measure the minerals in lignite need to be determined.

Many studies have dealt with the role of temperature in mineral phase transitions (Querol et al., 1994; Bryers, 1996; Ward et al., 2001; Ma et al., 2014; Zhang et al., 2015; Tao, 2015; Wen et al., 2016). For instance, calcite decomposes at 650 °C, gypsum transforms to anhydrite at 400 °C, illite decomposes at 900 °C, and kaolinite changes to meta-kaolinite at 325–450 °C and decomposes into amorphous SiO₂ and Al₂O₃ at 1000–1400 °C. The increase of ashing temperature mainly leads to a decrease in the crystal mineral content, an increase of amorphous mineral, and a transition of ash samples to the molten state. The changes in mineral and coal ash composition, focusing on the effects of coal combustion characteristics, ash melting characteristics, slagging and ash deposits, have been studied at different ashing temperatures (Nel et al., 2014; Li et al., 2017a, 2017b). However, little is known about the characteristics of the original mineral formation obtained by observing changes in the specific mineral species and content through rising ashing temperature. Coal with different substances will

* Corresponding author at: School of Resources and Geosciences, China University of Mining and Technology, Xuzhou 221116, China.

E-mail address: 15162186837@163.com (B. Wang).

<https://doi.org/10.1016/j.gexplo.2018.08.002>

Received 3 May 2018; Received in revised form 20 July 2018; Accepted 12 August 2018

Available online 14 August 2018

0375-6742/ © 2018 Elsevier B.V. All rights reserved.

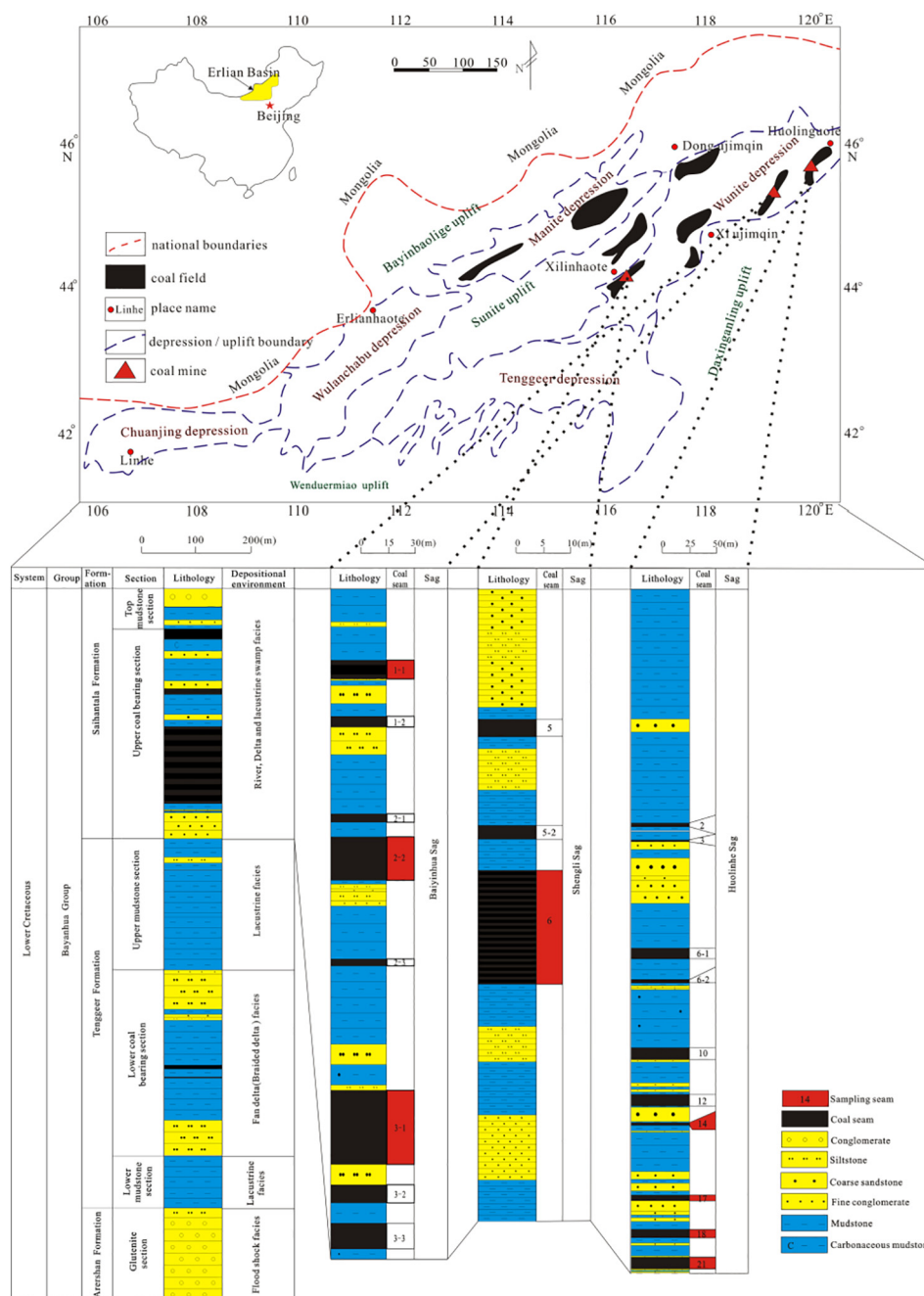


Fig. 1. Sampling locations and coal stratigraphy.

also affect the degree of ashing. For example, coal with high fixed carbon content and small volatile content, its peak temperature and activation energy are higher, coal combustion performance is poor, and the ashing time is longer, often increasing the loss rate of clay minerals (Ma et al., 2015). In view of this, It is necessary to study the mineral loss in the process of ashing coal with different substances, and then a prediction model suitable for coal with different substances was established for medium-temperature ash to obtain the low-temperature ash mineral composition.

For minerals that decompose easily, the ashing temperature affects analytical accuracy (Yang et al., 2016). For example, Na begins to escape at temperatures ranging from 400 °C to 600 °C. Ca precipitates slowly at temperatures below 600 °C, but precipitates faster after 1000 °C (Tao, 2015). At the same time, the change of ash temperature may also cause changes in the occurrence of elements. For example,

NaCl is the main existence form in the ash fired at temperatures between 500 °C and 600 °C. With the increase of ash temperature, there will be sodium feldspar at 700 °C and nepheline at 800 °C to 900 °C. The chemical composition of coal ash is one of the main factors affecting the sintering characteristics and ash fusion characteristics of coal ash (Wang et al., 2010). Therefore, understanding the variation characteristics of ash composition and the change of element occurrence state under different ashing temperatures are the basis for rationally solving the problem of ash accumulation and slagging.

Based on this problem, typical lignite samples from three coal mines in the Erlian Basin were selected. The raw coal of low- and middle-temperature ash were selectively leached, excluding the raw coal of high-temperature ash, and then ashed at different temperatures (< 200 °C, 500 °C, 815 °C). The minerals and ash products were analyzed by XRD, ash composition analysis, and mathematical methods to

Table 1
Coal sample details.

Coal sample	Output location of coal samples				Description
	Sag	Coal mine	Coal seam	Thickness/m	
B-1	Baiyinhua Sag	Baiyinhua No.3 open-pit mine	1–1	$\frac{2.02 - 7.60}{5.36}$	The coal is black, dark brown, brown, with light brown and brown streaks; luster has a weak asphalt gloss and is dark; weathered coal is not glossy. Coal seam 1–1 is dominated by dull coal with bright coalbands and is detrital coal. Coal seam 2–2 is dominated by bright coal with vitrain and dull coal band sand is xyloid coal. Coal seam 3–1 is dominated by bright and dull coal with some thin vitra in layers and small amounts of fusain; it is detrital coal. The bedding is horizontal and gentle wavy.
B-2			2–2	$\frac{0.4 - 19.79}{7.27}$	
B-3a			3–1	$\frac{2.23 - 39.84}{18.77}$	
S-6a S-6b	Shengli Sag	Shengli X-1 open-pit mine	6 6	$\frac{1.95 - 36.25}{17.41}$	The coal is generally puce, black-brown, brown, with light brown and brown streaks; luster has a weak asphalt gloss and dark luster; weathered coal is not glossy. Coal and rocks alternate; coal is detrital; vitrain and fusain are sandwiched between bright and dull coal in lenses or 3–5 mm and 1–3 mm, or occasionally 5 mm bands. The bedding is horizontal and gentle wavy.
H14	Huolinhe Sag	Open-pit mine south of Houlinhe	14	$\frac{1.1 - 12.8}{2.8}$	The coal is brown, brown-black, with brown or slight cinnamon streaks; dull pitchy and partly pitchy luster; lenticular, banded, and linear, or stratified structures; the coal and rock types are dominated by xyloid coal.
H-17			17	$\frac{1.1 - 16.4}{3}$	
H-18			18	$\frac{1.1 - 22}{4.8}$	
H-21			21	$\frac{1.1 - 26.6}{8.6}$	

Note: $\frac{\text{minimum} - \text{maximum}}{\text{average}}$.

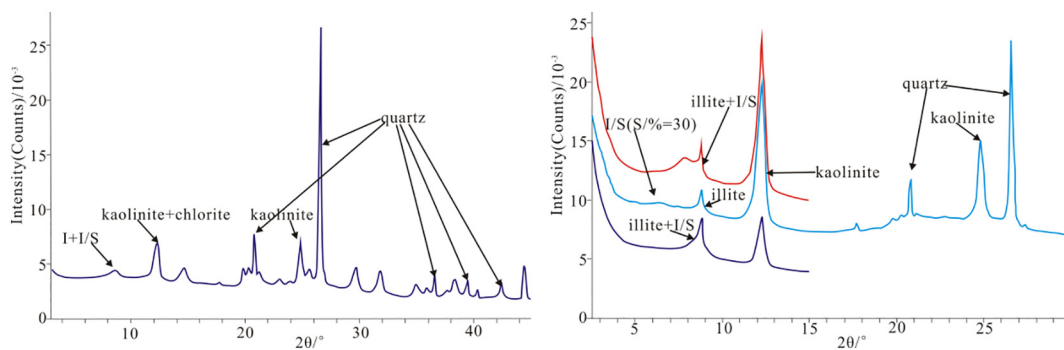


Fig. 2. Whole-rock and clay minerals XRD spectra of B-2 LTA.

Table 2
XRD data of LTA and MTA.

Coal sample number	Clay minerals/%					Quartz/%	Potassium feldspar/%	Carbonate/%	
	Kaolinite	Chlorite	Illite	I/S	Total			Calcite	Siderite
B-1 (LTA)	100	0	0	0	73	27	0	0	0
B-2 (LTA)	75	0	5	20	61	39	0	0	0
B-3a (LTA)	77	0	10	13	45	54	1	0	0
S-6a (LTA)	99	0	1	0	69	29	0	2	0
S-6b (LTA)	90	0	10	0	57	43	0	0	0
H-14 (LTA)	100	0	0	0	42	57	0	1	0
H-17 (LTA)	83	0	10	7	39	60	1	0	0
H-18 (LTA)	72	0	5	23	64	35	1	0	0
H-21 (LTA)	44	0	8	48	52	48	0	0	0
B-1 (LTA)	100	0	0	0	13	82	1	4	0
B-2 (LTA)	18	1	16	65	32	68	0	0	0
B-3a (LTA)	57	0	19	24	30	68	0	2	0
S-6a (LTA)	93	0	7	0	25	74	0	1	0
S-6b (LTA)	60	0	40	0	25	75	0	0	0
H-14 (LTA)	100	0	0	0	33	67	0	0	0
H-17 (LTA)	80	0	12	8	34	65	0	0	0
H-18 (LTA)	29	0	13	58	42	58	0	0	0
H-21 (LTA)	10	0	13	77	40	60	0	0	0

Note: I/S - illite/smectite mixed layer mineral.

Table 3
Rate of mineral change under heating conditions.

Coal sample number	Change rate/%			
	Clay minerals	Kaolinite	Illite	I/S
B-1	94.14	94.14	–	–
B-2	69.91	92.78	3.72	2.22
B-3a	47.06	60.81	–0.58	2.26
S-6a	85.80	86.66	0.61	–
S-6b	74.85	83.24	–0.58	–
H-14	33.16	33.16	–	–
H-17	19.53	22.44	3.43	8.03
H-18	60.40	84.05	–2.88	0.14
H-21	38.46	86.01	0.00	1.28
Average	58.15	71.48	0.53	2.79

Note: The positive and negative values represent mineral losses and increase with increasing ashing temperature, respectively.

explore the effect of ashing temperature and alkali or alkaline earth elements (AAEMS) on the degree of ashing. The conversion rates of clay minerals of lignite comprised different substances, and the low-temperature ash mineral compositions reversed by medium-temperature ash mineral composition were modeled based on the XRD data.

2. Coal sample, experiment, and data processing method

2.1. Coal samples and geological settings

The Erlian Basin is a Mesozoic rift basin on the Inner Mongolia–Daxinganling Hercynian fold basemen. It is located in

central-northern Inner Mongolia, China and is surrounded by the Daxinganling to the east, the Wulatehouqi to the west, the Yin Mountains to the south, and the China–Mongolia border to the north. The Erlian Basin is one of the largest onshore sedimentary basins in China and comprises five depressions and an uplift. The Erlian Basin has experienced five phases of tectonism since the Mesozoic.

Early Cretaceous is the main coal-forming period comprising three lake-forming periods and five depositional discontinuities. The lacustrine stage is represented by the early Aershan Formation and the Tenggeer Formation. The discontinuities document four stages in the evolution of the lake basins (inherited lake basin, early prevail of lake basin, late prevail lake basin, recession lake basin) (Huang et al., 2003; Ding et al., 2016).

From the bottom to the top, the Early Cretaceous Baiyanhua Group, is divided into the Aershan Formation, Tenggeer Formation, and Saihantala Formation. Delta and lake swamp facies are part of the Tenggeer and Saihantala Formations and are the main coal-bearing strata (Fig. 1). Because of the differences in the coal-forming environment in the various depressions, the coal seam structure varies spatially.

The upper coal-bearing section of the Saihanatala Formation from different mines in the Erlian Basin (Baiyinhua No.3 open-pit mine, Shengli X-1 open-pit mine, and open-pit mine south of Houlinhe) was studied. The samples represent three thick coal seams from Baiyinhua No.3 open-pit mine, the No.6 coal seam in the Shengli X-1 open-pit mine, and the No.14, No.17, No.18, and No.21 coal seams in the open-pit mine south of Houlinhe (Fig. 1).

Fresh coal samples were selected, and the physical characteristics are given in Table 1. Element and maceral analysis, R_o testing and industrial analysis were performed (Schedules 1 and 2). The results suggest that the sample is characterized by low–moderate ash content, low

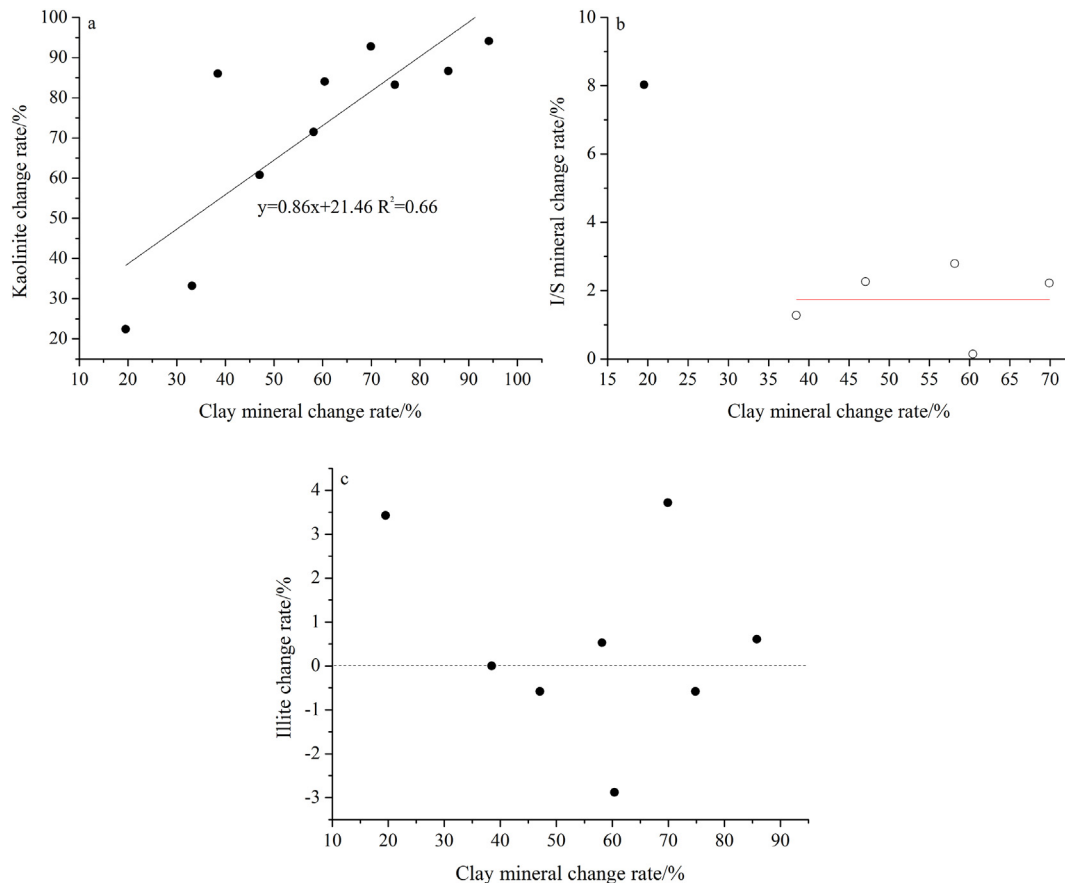


Fig. 3. Rate of change for kaolinite, illite, and illite/smectite with heating.

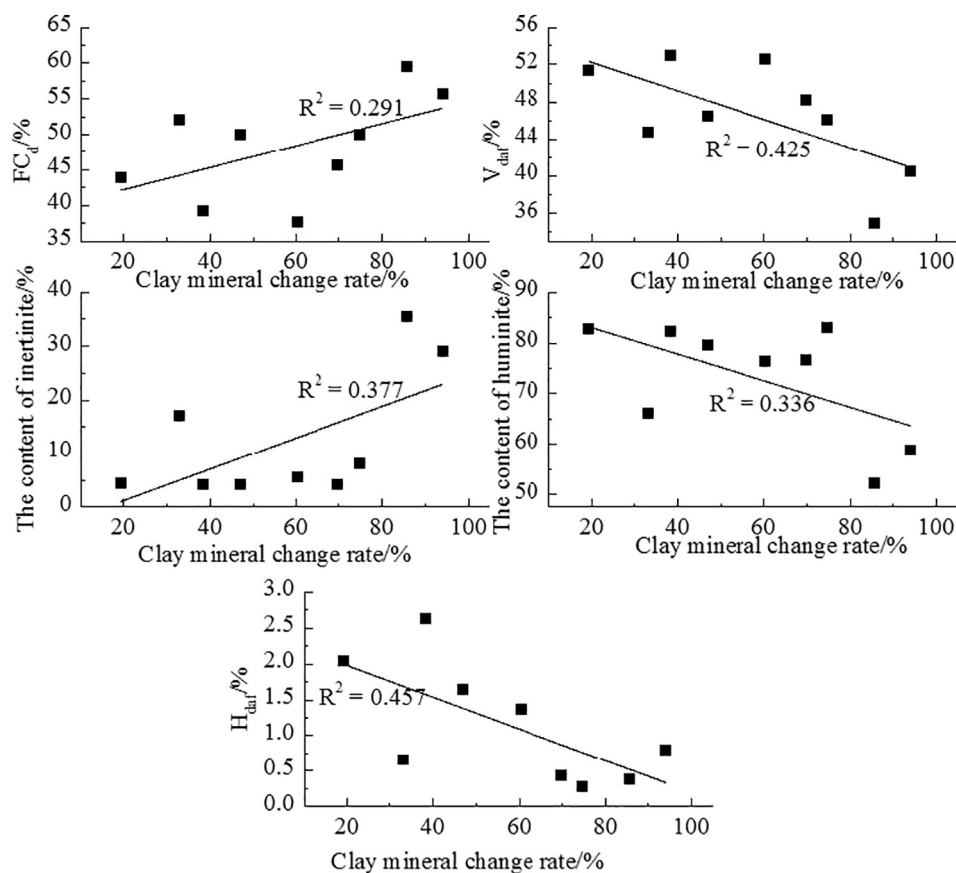


Fig. 4. Clay mineral loss rate vs. various controlling factors.

Table 4
Correlation coefficient matrix of the five indicators.

	V_{daf}	FC_{daf}	H_{daf}	Huminite	Inertinite
V_{daf}	1	-0.97	0.67	0.87	-0.91
FC_{daf}		1.00	-0.66	-0.78	0.83
H_{daf}			1.00	0.52	-0.51
Huminite				1.00	-0.96
Inertinite					1.00

sulfur content, and is young brown coal. Huminite content is high and dominated by ulminite, whereas the inertinite and liptinite contents are low. The inorganic macerals are mainly clay minerals and quartz.

2.2. Mineral enrichment methods in coal

Minerals in coal comprise non-mineral inorganics such as water-soluble salts, alkali or alkaline earth elements (AAEMS) combined with organic matter, and discrete minerals. In lignite, AAEMS during ashing

Table 5
Variance decomposition principal component extraction analysis result.

Component	Initial eigenvalue			Extraction load of square sum		
	Total	Variance %	Accumulate %	Total	Variance %	Accumulate %
1	4.108	82.152	82.152	4.108	82.152	82.152
2	0.611	12.219	94.371	0.611	12.219	94.371
3	0.237	4.735	99.106			
4	0.031	0.620	99.726			
5	0.014	0.274	100.000			

form sulfates or nitrates with organic sulfur and organic nitrogen and affect the ashing. Deionized water and ammonium acetate are used to remove the non-mineral inorganics from coal (Shang et al., 2016). Five grams of the coal sample are mixed with 100 ml of deionized water and stirred for 4 h at 60 °C. Then, the solid particles are washed with 100 ml deionized water and finally centrifuged. The residue is mixed with 100 ml of ammonium acetate solution at 60 °C and stirred for 4 h and then rinsed with deionized water until no ammonium acetate is left. The residual solids are collected and dried under vacuum at 50 °C for 24 h.

Low-temperature ash (LTA) is obtained by ashing the leached coal samples using an EMITECH K1050X plasma asher at < 200 °C until the mass difference is < 1%.

Middle-temperature ash (MTA) is obtained by following the GB/T 212–2008 standard test method. One gram of the leached coal sample is placed in a muffle furnace with the door open with a gap of about 15 mm. Then, the temperature of the muffle furnace is slowly increased to 500 °C in 30 min until the mass difference is < 1%.

High-temperature ash (HTA) is obtained by a process identical to MTA but by weighing 1 g of raw coal instead. The temperature of the

Table 6
Principal component analysis of total change rate of clay minerals.

Coal sample number	Clay minerals change rate/%	F ₁	F ₂
B-1	94.14	7.30	-13.75
B-2	69.91	35.32	-28.84
B-3a	47.06	34.26	-29.05
S-6a	85.8	-3.48	-9.53
S-6b	74.85	33.25	-29.96
H-14	33.16	19.93	-20.62
H-17	19.53	40.95	-29.41
H-18	60.4	40.63	-26.92
H-21	38.46	43.91	-28.51

Table 7
Component matrix.

Factor	Element	
	1	2
V _{daf}	0.983	-0.016
FC _d	-0.941	-0.051
H _{daf}	0.719	0.674
Huminite	0.922	-0.272
Inertinite	-0.943	0.283

muffle furnace is raised slowly to 500 °C within 30 min, maintained for 30 min, and then increased to 815 °C at 10 °C/min until the mass difference is < 1% (Yang et al., 2016).

2.3. Testing and data processing

Before ashing, the coal samples were separated into three parts to prepare three kinds of ash. The ash samples were milled and passed through a 200-mesh sieve. X-ray diffraction analysis of LTA and MTA was performed with a Bruker D8-DISCOVER X-ray diffractometer using 40 kV, 40 mA, and scanning angle of 3–45°. Relative clay content was determined by the suspension method. Clay minerals with diameter < 2 μm were extracted, and make directional film production, including natural air dry piece, ethylene glycol piece and 550 °C piece. Subsequently, diffraction peak intensity contrast method and adiabatic equations were used to calculate the clay mineral content (Fig. 2) (Jozanikohan et al., 2016). HTA was determined following the GB/T 1574-2007 standard test method and a Bruker S8 Tiger X-ray diffractometer, using a Rh tube at 4 kW and 67 mA (Table 2).

Since quartz undergoes the phase transition from α- to β-quartz at 573 °C (Song, 2011) and the ashing temperature of LTA and MTA is < 573 °C, the quartz content in coal should remain unchanged. XRD provides the relative content of minerals; therefore, the absolute mass

Schedule 1

Coal quality analysis result.

Coal sample number	Industrial analysis				Elemental analysis				Total sulfur	Formal sulfur		
	M _{ad} %	A _d %	V _{daf} %	FC _d %	O _{daf} %	C _{daf} %	H _{daf} %	N _{daf} %	S _{t,d} %	S _{p,d} %	S _{s,d} %	S _{o,d} %
B-1	29.78	6.58	40.46	55.63	24.51	72.96	0.79	1.55	0.17	0.01	0	0.16
B-2	34.62	11.81	48.21	45.67	26.4	70.86	0.42	1.25	0.95	0	0	0.95
B-3a	31.84	7.01	46.4	49.84	23.97	72.04	1.63	1.59	0.72	0	0	0.72
S-6a	30.42	8.42	34.95	59.57	21.83	76.49	0.38	1.07	0.22	0.03	0	0.19
S-6b	35.89	7.67	45.97	49.88	26.51	71.09	0.27	1.39	0.69	0.02	0	0.67
H14	32.59	6.1	44.66	51.97	23	74.63	0.66	1.48	0.21	0	0	0.21
H-17	29.18	9.91	51.38	43.8	22.38	73.37	2.04	1.44	0.69	0.03	0	0.66
H-18	29.78	20.36	52.65	37.71	22.82	72.5	1.36	1.63	1.35	0.03	0.01	1.31
H-21	26.88	16.79	52.93	39.17	20.56	72.81	2.63	1.84	1.79	0.11	0.03	1.65

Note: The letters B, S, and H represent Baiyinhua, Shengli, and Huolinhe, respectively.

ratio of the mineral change is derived based on this assumption.

$$\frac{Quartz_{LTA}(w,\%)}{Quartz_{MTA}(w,\%)} = \frac{m_{MTA}}{m_{LTA}} \quad (1)$$

$$\frac{m_{LTA}^{Mineral}}{m_{MTA}^{Mineral}} = \frac{Mineral_{LTA}(w,\%)}{Mineral_{MTA}(w,\%)} \cdot \frac{m_{LTA}}{m_{MTA}} = \frac{Mineral_{LTA}(w,\%)}{Mineral_{MTA}(w,\%)} \cdot \frac{Quartz_{MTA}(w,\%)}{Quartz_{LTA}(w,\%)} \quad (2)$$

Note: m_{MTA} : the absolute mass of MTA; $Mineral_{LTA}$ (wt%): relative mineral content of LTA

The factors affecting the change of clay minerals are analyzed by using principal component analysis. The quantitative XRD data for LTA and MTA are converted into elemental content based on the standard chemical formula of each mineral (Ward et al., 2001; Koukouzas et al., 2010) (Table 6). The elements in LTA and MTA are minerals that do not contain AAEMS or water-soluble salts. The standard procedure is to fix the SiO₂ content and use mass conservation to compare the ash composition at different ashing temperatures.

$$m(SiO_2) = c_{Si,LTA}A_{LTA} = c_{Si,MTA}A_{MTA} = c_{Si,HTA}A_{HTA} \quad (3)$$

Note: $m(SiO_2)$: the absolute mass of SiO₂, A_{LTA} : ash content of LTA, $c_{Si,LTA}$: relative SiO₂ content in LTA

3. Results and discussion

3.1. Ash mineralogy at different ashing temperatures

The main minerals in the coal seams from the Erlian Basin are clay minerals (55.78%) and quartz (43.55%). Carbonate minerals such as calcite are found in only a few coal seams. The clay minerals are mainly kaolinite (82.22%), mixed illite/smectite (12.33%), and illite (5.44%). The chlorite content is the least. The characteristics of clay minerals are attributed to the large amounts of humic acid in the lignite that is conducive to the formation of kaolinite.

At < 500 °C, the quartz content is constant, and Eqs. (1) and (2) are used to obtain the absolute mass ratio and the rate of change as a function of temperature for different minerals (Table 3). The results suggest that the increase in ashing temperature does not change the mineral species but only the relative ratio. The clay minerals decompose most during heating (19.53%–94.14%, 58.15% average) owing mainly to the loss of kaolinite (22.44%–94.14%, 71.48% average), followed by the loss of mixed illite/smectite (0.14%–8.03%, 2.19% average), whereas illite almost remains the same (-0.58%–3.72%, 0.53% average) (Fig. 3). The loss rate of kaolinite and clay minerals is positively correlated; with ashing temperature at 327 °C, kaolinite loses the interlayer water and changes into amorphous metakaolinite

Schedule 2
The result of quantitative determination of macerals and $R_{o,max}$

Coal sample number	Organic macerals/%													$R_{o,max}/\%$	
	Huminite/%						Inertinite/%								Liptinite/%
	Textinite	Ulminite	Attrinite	Desinite	Gelinite	Corphuminitite	Fusinite	Semi-fusinite	Macrinite	Micrinite	Sclerolinite	Inertodetrinite	Sporinite		
B-1	25.97	17.65	3.78	0.50	4.54	6.30	16.64	7.31	1.26	0.00	0.00	3.78	5.29		
B-2	23.04	33.06	8.27	1.75	7.01	3.51	2.00	0.50	0.00	0.50	0.00	1.00	8.52		
B-3a	7.98	32.86	6.76	1.54	18.73	11.67	2.15	0.00	0.61	0.00	0.00	1.23	7.98		
S-6a	14.18	23.38	2.98	0.50	7.71	3.23	16.42	6.96	3.98	1.99	1.24	4.97	3.98		
S-6b	14.78	38.44	12.63	5.38	7.26	4.57	5.38	1.34	0.81	0.00	0.00	0.54	3.23		
H14	6.11	34.86	8.83	2.49	9.28	4.53	8.37	1.36	1.36	1.36	1.58	2.94	7.70		
H-17	14.00	35.25	4.83	1.21	16.18	11.35	1.93	0.48	0.72	0.00	0.00	1.21	5.55		
H-18	5.80	33.16	8.57	1.93	18.52	8.29	3.04	0.55	0.55	0.00	0.00	1.38	8.84		
H-21	9.93	26.91	9.93	1.57	24.04	9.93	3.14	0.26	0.00	0.00	0.00	0.78	6.01		

Coal sample number	Inorganic component/%													$R_{o,max}/\%$
	Mineral composition/%													
	Cutinite	Resinite	Suberinite	Alginite	Liptodetrinite	Chlorophyllinite	Bituminite	Claymineral	Sulfide	Carbonate	Silicon-oxide	Other		
B-1	2.77	1.51	0.25	0.00	1.76	0.00	0.00	0.00	0.00	0.00	0.66	0.00	0.35	
B-2	5.26	3.01	0.75	0.00	1.25	0.00	0.00	0.00	0.00	0.00	0.56	0.00	0.32	
B-3a	3.68	2.15	0.61	0.00	1.54	0.00	0.00	0.00	0.00	0.00	0.51	0.00	0.32	
S-6a	2.49	1.24	0.25	0.00	0.99	0.00	0.00	2.18	0.44	0.00	0.87	0.00	0.3	
S-6b	2.96	0.81	0.00	0.00	0.81	0.00	0.00	0.00	1.08	0.00	0.00	0.00	0.34	
H14	3.40	2.72	0.00	0.00	2.49	0.00	0.00	0.00	0.00	0.00	0.64	0.00	0.32	
H-17	3.38	1.69	0.00	0.00	1.93	0.00	0.00	0.00	0.00	0.00	0.28	0.00	0.33	
H-18	4.70	1.93	1.11	0.00	1.11	0.00	0.00	0.00	0.00	0.00	0.26	0.00	0.27	
H-21	3.40	1.31	0.52	0.00	0.78	0.00	0.00	0.00	0.21	0.00	0.43	0.00	0.3	

($\text{Al}_2\text{O}_3 \cdot 2\text{SiO}_2 \cdot 2\text{H}_2\text{O}$ (kaolinite) \rightarrow $\text{Al}_2\text{O}_3 \cdot 2\text{SiO}_2$ (metakaolin) + $2\text{H}_2\text{O}$ (327–550 °C))(Yang et al., 2016). With the increase of ashing temperature, the illite/smectite mineral content also suffered a certain loss due to the process of losing interlayer water, but the loss rate of illite/smectite mineral is mainly < 4% with an average of 1.7% (Fig. 3b). Compared with the loss rate of kaolinite in the whole process, the loss rate of illite/smectite mineral is relatively low (Fig. 3a). Other minerals will not be elaborated here since their content is less in the coal and the experimental error is large.

3.2. Clay minerals loss rate

The variable coal composition controls the loss rate of clay minerals. As a result, the loss rate of clay minerals will vary as a function of the ashing temperature and coal composition.

The change rate of clay minerals and macerals, elemental composition, water content, and ash content were examined to investigate the main controlling factors of the loss of clay minerals owing to the increase in ashing temperature. The results suggest that the clay mineral conversion rate is related to FC_d , the content of inertinite, V_{daf} , H_{daf} , and huminite and is positively correlated with the first two (Fig. 4). Previous studies on lignite combustion have argued that the higher the fixed carbon content, the smaller the volatile content. Furthermore, the increase in the peak temperature and activation energy suggests that the combustion performance gradually deteriorates and coal ashing becomes more difficult (Ma et al., 2015). The higher the content of H and huminite in coal is, the more side chains the aromatic group has, and the more difficult coal combustion is. The higher the inertinite content is, the higher the content of aromatic compounds is, the more difficult coal ashing becomes and the longer it takes, and the loss of clay minerals such as kaolinite increases.

3.3. Mineral inversion model

The above analysis suggests that the clay mineral conversion rate is related to FC_d , the content of inertinite, V_{daf} , H_{daf} , and huminite. Subsequently, the principal component analysis of the change rate of clay minerals was carried out based on these five factors.

The results suggest that there are different degrees of correlation between the five indexes: V_{daf} , huminite, and H_{daf} are positively correlated, while FC_d is positively correlated with inertinite. Principal component analysis is necessary to minimize the loss of the original index information while reducing the index analysis (Table 4). SPSS software was used for the dimension reduction of independent variables. PCA suggests that the cumulative Eigen values of the first two principal components account for 94.371% of the total variance, with less contribution from subsequent principal component Eigen values. The effect on the clay minerals change rate is small (Table 5). Two principal components F_1 and F_2 are extracted, and the original data of the five indices are normalized to eliminate the effect of the different dimensions of the parameters (Table 6). Based on the correlation function analysis of F_1 , F_2 , and clay minerals change rate, the mathematical model of the clay minerals loss rate for lignite with variable composition is established.

$$F_1 = 0.48x_1 - 0.46x_2 + 0.35x_3 + 0.45x_4 - 0.47x_5 \quad (4)$$

$$F_2 = -0.02x_1 - 0.066x_2 + 0.862x_3 - 0.348x_4 + 0.361x_5 \quad (5)$$

$$Y = 66.838 - 1.654 F_1 - 1.564 F_2 \quad (R^2 = 0.41) \quad (6)$$

Note: Y is the change rate of the clay minerals; x_1 – x_5 are V_{daf} , FC_d , H_{daf} , and the content of huminite and inertinite, respectively.

As it can be inferred from Table 7, the first principal component (F_1) is positively correlated with V_{daf} and huminite (load > 0.9) and negatively correlated with FC_d and inertinite (load > 0.9). The second principal component mainly reflects H_{daf} , and the correlation with other factors is very low, suggesting that the clay minerals

transformation rate, FC_d , and inertinite are positively correlated and negatively correlated with V_{daf} , H_{daf} , and huminite (Table 7). This is in line with the above and suggests that the model is suitable for predicting the change rate of clay minerals in lignite.

The XRD data for LTA can be derived from the change rate of the clay minerals and the XRD data for MTA.

$$a = \frac{1}{1 + (1 - Y)\frac{d}{c}} \times 100\% \quad (7)$$

$$b = \left(1 - \frac{1}{1 + (1 - Y)\frac{d}{c}} \right) \times 100\% \quad (8)$$

$$m = \frac{100(1 - Y)n}{78.54 - 0.86Y} \times 100\% \quad (9)$$

$$k = \frac{100(1 - Y)p}{91.837 + 0.109Y} \times 100\% \quad (10)$$

$$l = (100 - m - k) \times 100\% \quad (11)$$

Note: a and c represent the quartz content in LTA and MTA, whereas b and d denote the clay minerals in MTA. Y is a conversion factor for clay minerals. m and n are the kaolinite contents in LTA and MTA. k and p are the content of illite/s

3.4. Ash composition

Previous studies have argued that silica exists in coal in the form of quartz and aluminosilicates. The melting points of these minerals are high and they will not release in the form of gas; therefore, SiO_2 at any temperature should remain constant (Yang et al., 2016). The SiO_2 content of LTA and MTA is converted through the method shown in Section 2.3, which is higher than that of HTA. The reason is that the non-mineral inorganics in LTA and MTA are ignored. As the loss of clay minerals will lead to the reduction of ash yield from low to medium temperatures, it is assumed that Si exists in the form of crystalline minerals in raw coal and that the SiO_2 content in the unit mass of coal is fixed to remove the effect of ash yield owing to the different ashing temperatures. Eq. (3) is used to standardize the elements, and the calculation results are presented in Schedule 3.

Al_2O_3 in coal is mainly in clay minerals. Al_2O_3 in LTA, MTA, or HTA show good correlation and, with the increase in temperature, alumina in coal is difficult to precipitate because of the high melting point of the aluminosilicates (Fig. 5a). With increasing temperature, Al_2O_3 in ash increases then decreases and finally increases. The values of Al_2O_3 in LTA and HTA are similar ($R^2 > 0.937$), suggesting that low-temperature ashing ensures the integrity of the clay minerals in coal, whereas medium-temperature ashing causes the partial loss of clay minerals.

The minerals in low-rank coal are discrete minerals, water-soluble salts in pore water, and organic compounds that form organometallic complexes. In low-rank coal, the last two account for most of the mineral components (Kiss and King, 1977; Given and Spackman, 1978; Kiss and King, 1979; Benson and Holm, 1985; Ward, 1991; Ward, 1992; Ward, 2002). AAEMS includes K, Na, Ca, and Mg. In this paper, the AAEMS reversed by LTA and MTA contains only elements rich in discrete minerals, such as K in illite, which represents the sum of the different occurrence characteristics in HTA. Both Na_2O and MgO have good correlation with low- and medium-temperature ashing data but differ at high temperatures (Fig. 5b and c). Elements present indiscrete minerals only account for 1.81% and 3.22% of the total despite the weak correlation of CaO with the three temperature regimes (Fig. 5e). The low- and medium- temperature ashing data are far less than the high-temperature ones, suggesting that AAEMS in coal mostly exist by combining with organic substances. However, K_2O in coal well correlates with LTA, HTA, and MTA and K in discrete minerals account for 49.86% of the total; thus, compared to alkaline earth elements, K in

Schedule 3

The ash composition of LTA, MTA and HTA.

Coal sample number	XRD mineral transformation and high temperature ash data								Ash yield/%		Normalized data				
	SiO ₂ /%	Al ₂ O ₃ /%	Fe ₂ O ₃ /%	MgO/%	CaO/%	Na ₂ O/%	K ₂ O/%			Al ₂ O ₃ /‰	Fe ₂ O ₃ /‰	MgO/‰	CaO/‰	Na ₂ O/‰	K ₂ O/‰
B-1 (LTA)	67.883	32.117	0.000	0.000	0.000	0.000	0.000	2.753	8.842	0.000	0.000	0.000	0.000	0.000	0.000
B-2 (LTA)	73.973	24.838	0.000	0.121	0.084	0.092	0.892	8.457	21.005	0.000	0.102	0.071	0.078	0.078	0.754
B-3a (LTA)	80.633	18.341	0.000	0.057	0.040	0.043	0.887	4.458	8.176	0.000	0.025	0.018	0.019	0.019	0.395
S-6a (LTA)	68.278	30.425	0.000	0.000	1.227	0.000	0.069	5.356	16.295	0.000	0.000	0.657	0.000	0.000	0.037
S-6b (LTA)	75.329	24.116	0.000	0.000	0.000	0.000	0.554	4.061	9.793	0.000	0.000	0.000	0.000	0.000	0.225
H-14 (LTA)	81.703	17.711	0.000	0.000	0.586	0.000	0.000	4.206	7.449	0.000	0.000	0.246	0.000	0.000	0.000
H-17 (LTA)	83.234	16.024	0.000	0.026	0.018	0.020	0.677	7.579	12.144	0.000	0.020	0.014	0.015	0.015	0.513
H-18 (LTA)	72.277	26.150	0.000	0.146	0.102	0.111	1.214	17.341	45.347	0.000	0.253	0.176	0.193	0.193	2.105
H-21 (LTA)	78.431	19.397	0.000	0.241	0.167	0.183	1.580	14.293	27.724	0.000	0.344	0.239	0.262	0.262	2.259
B-1 (MTA)	92.0271	5.5190	0.0000	0.0000	2.2786	0.0000	0.1754	2.0308	1.1208	0.0000	0.0000	0.4627	0.0000	0.0000	0.0356
B-2 (MTA)	86.8536	11.0413	0.1268	0.2588	0.1359	0.1487	1.4348	7.2029	7.9530	0.0913	0.1864	0.0979	0.1071	1.0335	
B-3a (MTA)	86.2546	11.5590	0.0000	0.0689	1.1908	0.0525	0.8742	4.1674	4.8171	0.0000	0.0287	0.4963	0.0219	0.3643	
S-6a (MTA)	89.0649	10.2007	0.0000	0.0000	0.5706	0.0000	0.1637	4.1058	4.1882	0.0000	0.0000	0.2343	0.0000	0.0672	
S-6b (MTA)	89.2967	9.7793	0.0000	0.0000	0.0000	0.0000	0.9240	3.4257	3.3501	0.0000	0.0000	0.0000	0.0000	0.3165	
H-14 (MTA)	86.3336	13.6664	0.0000	0.0000	0.0000	0.0000	0.0000	3.9800	5.4393	0.0000	0.0000	0.0000	0.0000	0.0000	
H-17 (MTA)	85.6276	13.7903	0.0000	0.0264	0.0184	0.0201	0.5173	7.3669	10.1592	0.0000	0.0194	0.0135	0.0148	0.3811	
H-18 (MTA)	82.7562	15.0263	0.0000	0.2314	0.1610	0.1760	1.6491	15.1455	22.7582	0.0000	0.3504	0.2438	0.2666	2.4976	
H-21 (MTA)	83.7804	13.5973	0.0000	0.2900	0.2017	0.2206	1.9100	13.3804	18.1937	0.0000	0.3880	0.2699	0.2952	2.5556	
B-1 (HTA)	28.4027	17.8510	3.8551	8.3753	39.4679	1.9074	0.1406	6.5800	11.7460	2.5366	5.5110	25.9699	1.2550	0.0925	
B-2 (HTA)	52.9718	28.9000	2.8969	2.2124	10.0113	1.6363	1.3713	11.8100	34.1309	3.4213	2.6129	11.8233	1.9325	1.6194	
B-3a (HTA)	51.2782	24.2099	4.0801	2.4235	12.5026	3.8030	1.7026	7.0100	16.9711	2.8602	1.6989	8.7644	2.6659	1.1936	
S-6a (HTA)	43.4305	27.7860	2.0156	7.3234	12.9691	6.1558	0.3197	8.4200	23.3958	1.6972	6.1663	10.9199	5.1832	0.2692	
S-6b (HTA)	39.8834	24.0222	3.3504	7.8994	13.2197	10.6156	1.0092	7.6700	18.4250	2.5698	6.0589	10.1395	8.1422	0.7741	
H-14 (HTA)	56.3296	10.4584	2.8605	2.0893	19.4730	8.5686	0.2207	6.1000	6.3796	1.7449	1.2745	11.8785	5.2268	0.1346	
H-17 (HTA)	63.6542	21.0506	1.7199	0.7738	8.2085	3.0739	1.5190	9.9100	20.8612	1.7045	0.7669	8.1347	3.0462	1.5053	
H-18 (HTA)	61.5613	26.8058	4.9652	0.5699	2.4555	1.8825	1.7598	20.3600	54.5766	10.1092	1.1603	4.9994	3.8329	3.5829	
H-21 (HTA)	66.7666	22.0959	2.7386	0.8289	2.9364	2.0097	2.6240	16.7900	37.0990	4.5980	1.3916	4.9302	3.3742	4.4057	

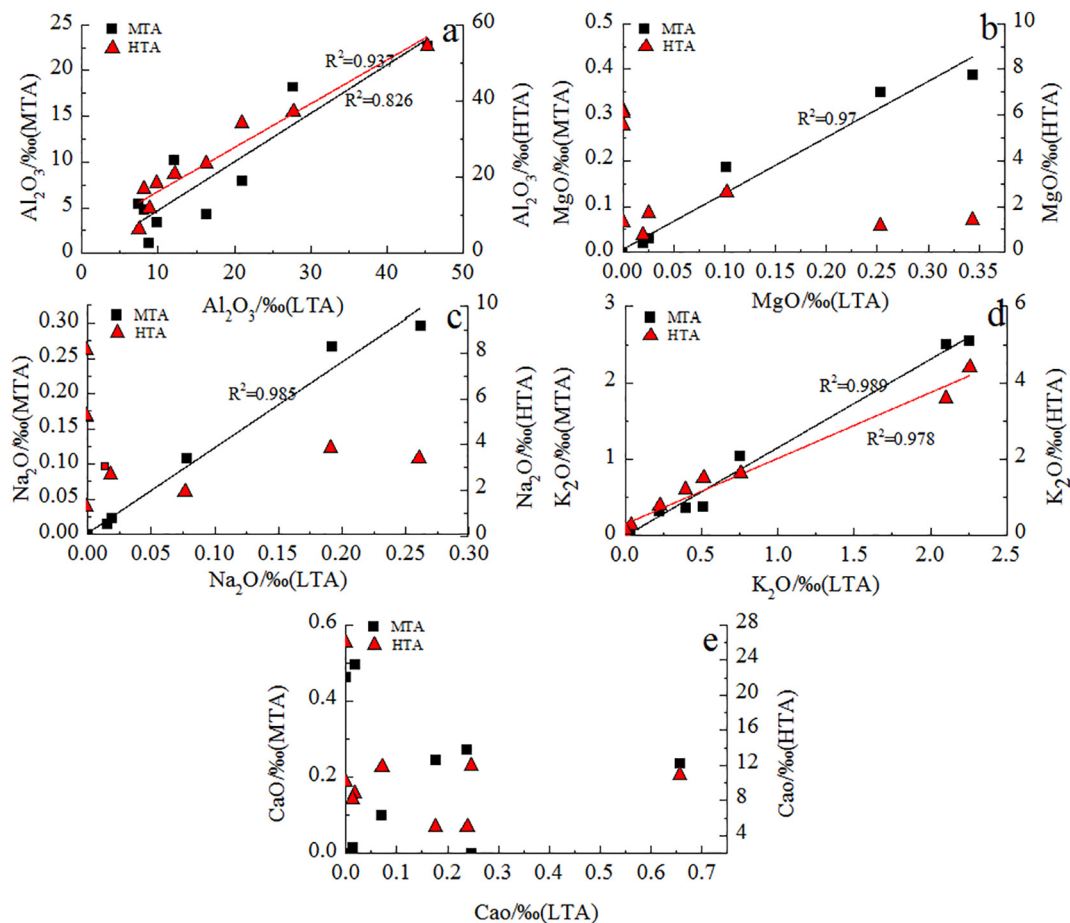


Fig. 5. Ash composition correlations for LTA, MTA, and HTA.

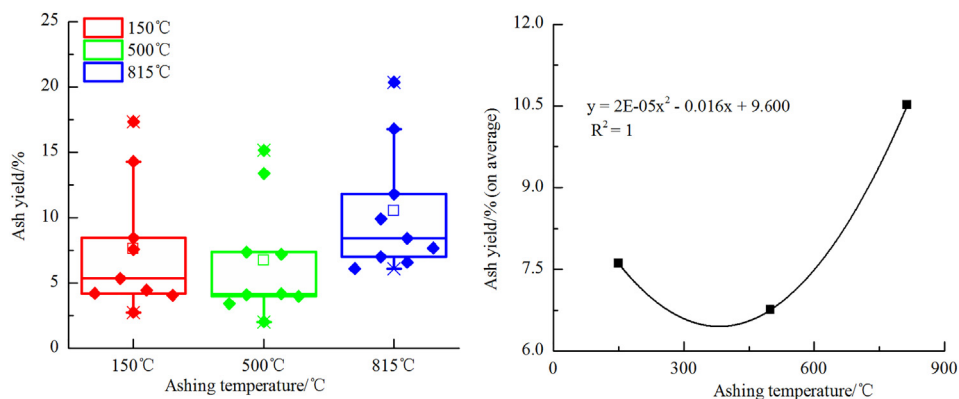


Fig. 6. Ash yield vs. ashing temperature.

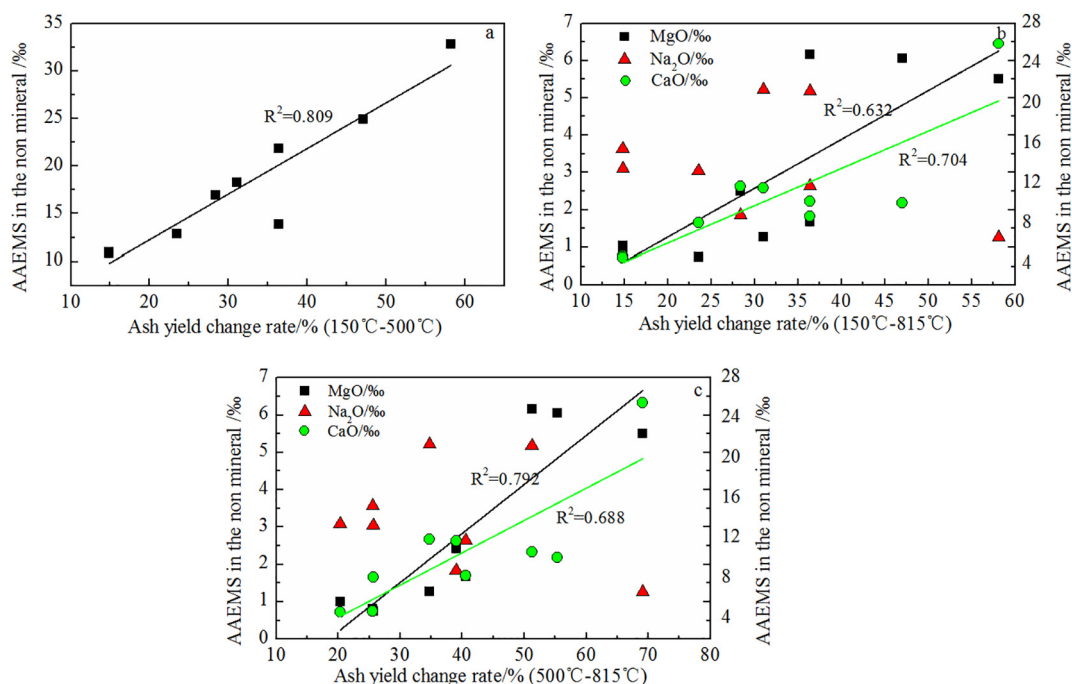


Fig. 7. Change rate of ash yield and AAEMS in non-mineral inorganics.

coal is mostly in clay minerals (Fig. 5d).

3.5. Ash yield

The selective leaching method was used to remove the water-soluble salts and the AAEMS of non discrete minerals in coal (LTA and MTA). Based on the ash composition at high temperature, Si, Al, Fe, and AAEMS oxides are expected in coal. K in AAEMs mainly occurs in clay minerals, whereas other elements combine with organic substances.

The ash yield (average 10.51%) of HTA was much higher than that of MTA (6.75%) and LTA (7.61%). The ash yield changes parabolically from high to low to high with increasing ashing temperature (Fig. 6). As the ashing temperature increases, a large amount of clay minerals is lost, and the loss of crystalline water leads to decreasing ash yield. However, for HTA, amorphous materials such as AAEMS react with each other or minerals to form new minerals. For example, sodium can react with aluminosilicates and free silica, but it can be converted to nonvolatile forms and deposited in ash, leading to ash yield that is much higher than that of LTA and MTA (Luo, 2016).

The AAEMS in non-mineral inorganics affects the rate of change of the ashing yield from low to high temperature. The ash yield change rate positively correlates with Ca and Mg and weakly with Na,

suggesting that Ca and Mg in lignite are important elements for controlling the ashing yield, with Ca being dominant. The same trends are seen from MTA to HTA but with increased effect for Mg (increase in R^2). In contrast, the effect of Ca is weaker (Fig. 7). Apparently, Ca and Mg in non-mineral inorganics can form new minerals during ashing but not the original minerals in coal. AAEMS in non-mineral inorganics positively affects the ash yield than the negative effect of elevated ashing temperature. In low-temperature ashing, the AAEMS in non-mineral inorganics will form sulfates or nitrates after reacting with organic sulfur or organic nitrogen, and this affects the ashing results. The sulfur in the Inner Mongolia lignite is mainly organic and contains large amounts of Ca and Mg associated with organic matter. Therefore, the use of leaching, LTA, and XRD is the most effective method to analyze Inner Mongolia lignite.

4. Conclusions

The minerals in coal seams from the Erlian Basin are mainly clay minerals and quartz, and minor calcite. The clay minerals are kaolinite, illite/smectite, and illite. Ashing temperatures < 500 °C do not cause changes in the mineralogy, only the proportions. Different degrees of loss occur to clay minerals during heating below 500 °C; that is,

kaolinite transforms into amorphous metakaolin after losing the inter-layer water, whereas illite and illite/smectite do not change.

The conversion rate of clay minerals is positively correlated with FC_d and inertinite, and negatively correlated with V_{daf} , H_{daf} , and huminite. Principal component analysis is used to extract the F_1 and F_2 principal components and a prediction model for the loss rate of the lignite clay minerals is established. The prediction model for the LTA mineral composition reversed by the MTA mineral composition is established using the loss rate of clay minerals as a bridge.

Al_2O_3 in coal is mainly present in clay minerals. Heating will decrease the clay minerals, whereas low-temperature ashing does not affect them. Lignite contains a large amount of AAEMS, in which Ca, Na, and Mg combine with organic oxygen-containing functional groups or other organic functional groups to form organometallic complexes. K mainly occurs in clay minerals.

AAEMS in non-mineral inorganics positively affects the ash yield more than the ashing temperature. Ca controls the degree of ashing at LTA below 500 °C. With increasing ashing temperature, the effect of Mg on the degree of ashing is enhanced but does not exceed that of Ca. The use of leaching, LTA, and XRD is the most effective method for analyzing the lignite mineral content.

Acknowledgments

The project was financially supported by the Key Laboratory of Coalbed Methane Resources and Reservoir Formation Process of the Ministry of Education (China University of Mining and Technology) (No.2018-005), the Fundamental Research Funds for the Central Universities (2015XKZD07), and National Science and Technology Major Project (2016ZX05041-001).

References

- Benson, S.A., Holm, P.L., 1985. Comparison of inorganics in three low-rank coals. *Ind. Eng. Chem. Prod. Res. Dev.* 24, 145–149.
- Bryers, R.W., 1996. Fireside slagging, fouling, and high-temperature corrosion of heat-transfer surface due to impurities in steam-raising fuels. *Prog. Energy Combust.* 22, 29–120.
- Cao, Y., Li, H., 1994. Study of low-temperature ashing of minerals in coal from Dongsheng coalfield, North-eastern margin of Ordos basin. In: *Bulletin of the 562 Comprehensive Geological Brigade Chinese Academy of Geological Sciences*. 5. pp. 225–235 (in Chinese).
- Ding, X., Liu, G., Zha, M., Gao, C., Huang, Z., Qu, J., Huang, Z., Qu, J., Lu, X., Wang, P., Chen, Z., 2016. Geochemical characterization and depositional environment of source rocks of small fault basin in Erlian Basin, northern China. *Mar. Pet. Geol.* 69, 231–240.
- Given, P.H., Spackman, W., 1978. Reporting of analyses of low-rank coals on the dry, mineral-matter-free basis. *Fuel* 57 (319–319).
- Harvey, R.D., Ruch, R.R., 1984. Overview of mineral matter in US coals. *ACS Div. Fuel Chem.* 29, 2–8.
- Harvey, R.D., Ruch, R.R., 1986. Mineral matter in Illinois and other US coals. *ACS Symp. Ser.* 301, 10–40.
- Huang, H., Jin, G., Lin, C., Zheng, Y., 2003. Origin of an unusual heavy oil from the Baiyinchagan depression, Erlian basin, northern China. *Mar. Pet. Geol.* 20, 1–12.
- Jozanikohan, G., Sahabi, F., Norouzi, G.H., Memarian, H., Moshiri, B., 2016. Quantitative analysis of the clay minerals in the Shurijeh Reservoir Formation using combined X-ray analytical techniques. *Russ. Geol. Geophys.* 57, 1048–1063.
- Kiss, L.T., King, T.N., 1977. The expression of results of coal analysis: the case for brown coals. *Fuel* 56, 340–341.
- Kiss, L.T., King, T.N., 1979. Reporting of low-rank coal analysis—the distinction between minerals and inorganics. *Fuel* 58, 547–549.
- Koukouzas, N., Ward, C.R., Li, Z., 2010. Mineralogy of lignites and associated strata in the Mavropigi field of the Ptolemais Basin, northern Greece. *Int. J. Coal Geol.* 81, 182–190.
- Li, N., Li, Y., Ban, Y., Song, Y., Zhi, K., Teng, Y., He, R., Zhou, H., Liu, Q., Qi, Y., 2017a. Direct production of high hydrogen syngas by steam gasification of Shengli lignite/chars: remarkable promotion effect of inherent minerals and pyrolysis temperature. *Int. J. Hydrogen Energ.* 42, 5865–5872.
- Li, J., Zhu, M., Zhang, Z., Zhang, K., Shen, G., Zhang, D., 2017b. Effect of coal blending and ashing temperature on ash sintering and fusion characteristics during combustion of Zhundong lignite. *Fuel* 195, 131–142.
- Luo, K., 2016. Transformation of AAEMS and Its Influence on Reactivity During Char Gasification With H_2O/CO_2 . Doctoral Dissertation. Taiyuan University of Technology, Tai Yuan (in Chinese).
- Ma, Y., Huang, Z., Tang, H., Wang, Z., Zhou, J., Cen, K., 2014. Mineral conversion of Zhundong coal during ashing process and the effect of mineral additives on its ash fusion characteristics. *J. Fuel Chem. Technol.* 42, 20–25 (in Chinese).
- Ma, S., Liu, X., Dai, J., Dai, C., Liu, X., Liang, L., 2015. Combustion performance of semi-coke from Inner Mongolia lignite under mild pyrolysis conditions. *J. China Coal Soc.* 40, 1153–1159.
- Nel, M.V., Strydom, C.A., Schobert, H.H., Beukes, J.P., Bunt, J.R., 2014. Reducing atmosphere ash fusion temperatures of a mixture of coal-associated minerals—the effect of inorganic additives and ashing temperature. *Fuel Process. Technol.* 124, 78–86.
- Querol, X., Fernandez Turiel, J.L., Lopez Soler, A., 1994. The behaviour of mineral matter during combustion of Spanish subbituminous and brown coals. *Mineral. Mag.* 58, 119–133.
- Shang, X., Hou, K., Wu, J., Zhang, Y., Liu, J., Qi, J., 2016. The influence of mineral matter on moisture adsorption property of Shengli lignite. *Fuel* 182, 749–753.
- Song, D., 2011. Quantitative and Occurrence Characteristics of Minerals in Coal. China University of Mining and Technology Press, Xu Zhou, Jiang Su, China, pp. 24–54 (in Chinese).
- Tao, Y., 2015. Basic Research on Combustion Characteristics and Ash Behaviors of High-alkali Zhundong Coal. Zhejiang University (in Chinese).
- Wang, Q., Jing, N., Luo, Z., Li, X., Jie, T., 2010. Experiments on the effect of chemical components of coal ash on the sintering temperature. *J. China Coal Soc.* 35, 1015–1020.
- Ward, C.R., 1978. Mineral matter in Australian bituminous coals. *Proc. Aust. Inst. Min. Metal.* 267, 7–25.
- Ward, C.R., 1991. Mineral matter in low-rank coals and associated strata of the Mae Moh basin, northern Thailand. *Int. J. Coal Geol.* 17, 69–93.
- Ward, C.R., 1992. Mineral matter in Triassic and Tertiary low-rank coals from South Australia. *Int. J. Coal Geol.* 20, 185–208.
- Ward, C.R., 2002. Analysis and significance of mineral matter in coal seams. *Int. J. Coal Geol.* 50, 135–168.
- Ward, C.R., Taylor, J.C., 1996. Quantitative mineralogical analysis of coals from the Callide Basin, Queensland, Australia using X-ray diffractometry and normative interpretation. *Int. J. Coal Geol.* 30, 211–229.
- Ward, C.R., Taylor, J.C., Matulis, C.E., Dale, L.S., 2001. Quantification of mineral matter in the Argonne Premium Coals using interactive Rietveld-based X-ray diffraction. *Int. J. Coal Geol.* 46, 67–82.
- Wen, C., Gao, X., Xu, M., 2016. A CCSEM study on the transformation of included and excluded minerals during coal devolatilization and char combustion. *Fuel* 172, 96–104.
- Yang, Y., Yang, X., Liu, Q., Zhang, H., Lv, J., 2016. Effect of ashing temperature on analysis of Zhundong coal ash. *J. China Coal Soc.* 41, 2441–2447 (in Chinese).
- Zhang, H.R., Bai, J., Kong, L.X., Li, X.M., Bai, Z.Q., Li, W., 2015. Behavior of minerals in typical Shanxi coking coal during pyrolysis. *Energy Fuel* 29, 6912–6919.